Anisotropy of the Taylor scale and the correlation scale in plasma sheet magnetic field fluctuations as a function of auroral electrojet activity

James M. Weygand,[1] W. H. Matthaeus,[2] M. El-Alaoui,[1] S. Dasso,[3] and M. G. Kivelson[1]

Received 24 March 2010; revised 28 July 2010; accepted 28 September 2010; published 23 December 2010.

[1] Magnetic field data from the Cluster spacecraft in the magnetospheric plasma sheet are employed to determine the correlation scale and the magnetic Taylor microscale from simultaneous multiple-point measurements for multiple intervals over a range of mean magnetic field directions for three different levels of geomagnetic activity. We have determined that in the plasma sheet the correlation scale along the mean magnetic field direction decreases from 19,500 ± 2200 to 13,100 ± 700 km as the auroral electrojet activity increases from quiet (<80 nT) to active conditions (>200 nT). The reverse occurs for the correlation scale perpendicular to the magnetic field, which increases from 8200 ± 600 km to 13,000 ± 2100 km as the auroral electrojet activity increases from quiet to active conditions. This variation of the correlation scale with geomagnetic activity may mean either a change in the scale size of the turbulence driver or may mean a change in the predominance of one over another type of turbulence driving mechanism. Unlike the correlation scale, the Taylor scale does not show any clear variation with geomagnetic activity. We find that the Taylor scale is longer parallel to the magnetic field than perpendicular to it for all levels of geomagnetic activity. The correlation and Taylor scales may be used to estimate the effective magnetic Reynolds numbers separately for each angular channel. Reynolds numbers were found to be approximately independent of the angle relative to the mean magnetic field. These results may be useful in magnetohydrodynamic modeling of the magnetosphere and can contribute to our understanding of energetic particle diffusion in the magnetosphere.

Citation: Weygand, J. M., W. H. Matthaeus, M. El-Alaoui, S. Dasso, and M. G. Kivelson (2010), Anisotropy of the Taylor scale and the correlation scale in plasma sheet magnetic field fluctuations as a function of auroral electrojet activity, *J. Geophys. Res.*, *115*, A12250, doi:10.1029/2010JA015499.

1. Introduction

[2] In the cascade picture of broadband turbulence, energy resides mainly at large scales but is transferred across scales by nonlinear processes, eventually reaching small scales where dissipation mechanisms of kinetic origin limit the transfer of energy, dissipate the fluid scale motions, and deposit heat. This general picture is expected in hydrodynamics and in fluid plasma models such as magnetohydrodynamics (MHD), when the associated Reynolds number and magnetic Reynolds number are large compared to unity, implying that nonlinear couplings are much stronger than the dissipation processes at large scales and that structures having a wide range of spatial scales will be involved in the dynamics. A broadband character is found in fluctuations of the magnetic field (and other quantities such as velocity and density) in the solar wind and in the plasma sheet. Many studies of turbulence in these systems [*Borovsky et al.*, 1997; *Tu and Marsch*, 1995; *Goldstein et al.*, 1994, 1995] analyze the cascade process through spectral analysis or through analysis of structure functions at various orders. Such analysis emphasizes the self-similar range of scale properties that give rise to descriptions such as the famous power law of Kolmogorov theory for fluids [*Kolmogorov*, 1941] and its variants in plasma [*Kraichnan*, 1965]. In hydrodynamics, the self-similar range is typically defined as extending from an energy-containing scale down to a Kolmogorov dissipation scale. Thus, the two most studied length scales are those that define the long wavelength and short wavelength ends of the power law inertial spectral range. The energy-containing scale λ_{CS} is typically of the same order as the correlation scale, which can be computed from time series data in a magnetized plasma using classical methods based on the assumption of Taylor frozen-in flow. The dissipation scale L_{diss} in hydrodynamics is the scale at

[1]Institute of Geophysics and Planetary Physics, University of California, Los Angeles, California, USA.
[2]Bartol Research Institute and Department of Physics and Astronomy, University of Delaware, Newark, Delaware, USA.
[3]Instituto de Astronomía y Física del Espacio (IAFE) and Departmento de Física, Facultad de Ciencias Exactas y Naturales, Universidad de Buenos Aires, Argentina.

0148-0227/10/2010JA015499

which the turbulent cascade is critically damped and significant energy is deposited into heat. Another scale, the magnetic Taylor microscale can be defined as

$$\lambda_T = \sqrt{\langle b^2 \rangle / \left\langle (\nabla \times b)^2 \right\rangle}, \quad (1)$$

where b is the magnetic field fluctuation vector for a suitably defined averaging procedure $\langle \ldots \rangle$. Note that λ_T is a length associated with the mean square spatial derivatives of b. In earlier work examining turbulence in the solar wind and plasma sheet [*Weygand et al.*, 2007, 2009a; *Matthaeus et al.*, 2008], we employ the equivalent definition that the Taylor scale is the length scale associated with the second derivative of the two-point magnetic field correlation function evaluated at zero separation, i.e., the radius of curvature at the origin [*Batchelor*, 1970]. With these definitions, one expects that, with the scale Reynolds number, given as $R = u\lambda_{CS}/\nu$, the Taylor and correlation scales are related by [*Batchelor*, 1970]

$$R_{\text{eff}} = \left(\frac{\lambda_{CS}}{\lambda_T}\right)^2. \quad (2)$$

[3] *Borovsky et al.* [1997] and *Weygand et al.* [2005, 2006] have shown that the magnetospheric plasma sheet magnetic field fluctuations display properties associated with turbulence. The electromagnetic energy that will eventually drive the plasma sheet turbulence is initially stored in the magnetotail lobes and transferred to the plasma sheet. The dominant mechanism for this transport is most likely reconnection. Understanding the turbulent magnetic fluctuations is important for understanding the physics of the transport of lobe electromagnetic energy and mass to the plasma sheet. However, measurements to ascertain the role of plasma sheet turbulence in energy transport remain incomplete. One of the key characteristics that have not yet been thoroughly studied is how the significant length scales of the turbulent energy cascade depend on the level of geomagnetic activity.

[4] Assuming a mapping between wave vectors and frequencies, the critical length scales are often identified in power spectral density plots as breaks in the spectral index. In the studies of *Borovsky et al.* [1997], *Neagu et al.* [2002], and *Weygand et al.* [2005, 2007, 2009a], the largest scales of the turbulent power spectral density plots, which are the correlation scales, were determined. However, only *Weygand et al.* [2005] commented on how the correlation scale varies as a function of geomagnetic activity. *Borovsky et al.* combined data from a number of plasma sheet events observed by the ISEE 2 Fast Plasma Experiment and found the autocorrelation cutoff time from the magnetic field measurements. Using the root mean square flow velocity, they converted the cutoff time into a spatial distance and reported values of about 10,000 km. *Neagu et al.* [2002] repeated the same procedure using AMPTE/IRM magnetic field and plasma data and determined a value of about 5000 km. *Weygand et al.* [2005] examined in detail four plasma sheet events observed by the Cluster spacecraft at times characterized by three different levels of geomagnetic activity. They found that the correlation scale varied between 1900 km (0.3 R_E) and 64,000 km (10 R_E); the shortest correlation scales were associated with moderate to high geomagnetic activity. *Weygand et al.* [2005] suggested that these correlation scales are limited along the Z axis of the GSM coordinates system by the plasma sheet thickness but did not comment on the limitation of the scales along the X and Y-GSM axes. *Weygand et al.* [2007] used a different approach to the determination of the correlation scale. They used two point cross-correlation measurements obtained over a range of spacecraft spatial separations to derive a cross correlation function and get the correlation scale. That work did not need to assume that the magnetic field fluctuations were frozen into the flow but did assume that the turbulent magnetic field fluctuations had the same properties for each of the approximate 100 plasma sheet events used in the study. With the large number of plasma sheet events *Weygand et al.* [2007] provided the first determination of the Taylor scale value in the plasma sheet. *Weygand et al.* [2009a, 2009b] subdivided the cross-correlation values into angular bins based on the angle between the spacecraft separation vector and the mean magnetic field direction. That work found that the correlation scale was longest in the direction along the mean magnetic field direction with a value of about 16,400 km (2.6 R_E) and shortest in the perpendicular direction at about 9200 km (1.4 R_E). A similar level of anisotropy was obtained for the Taylor scale values. The latter two *Weygand et al* studies combined all the plasma sheet intervals without regard to the level of geomagnetic activity. The present study sorts the data by levels of geomagnetic activity and obtains activity-dependent correlation scales.

[5] The fact that the correlation scale varies with the angle relative to the mean the magnetic field direction [*Weygand et al.*, 2009a] suggests that the driving mechanism or the scale size of the driving mechanism for the turbulent fluctuations varies with the direction relative to the magnetic field. It has been shown within the solar wind that the correlation scale length also varies with the direction relative to the mean magnetic field and this feature has been attributed to the superposition of two different types of turbulence, Alfvén wave turbulence and the quasi-two-dimensional turbulence [*Matthaeus et al.*, 1990]. In Alfvén wave turbulence, the wave vectors are aligned with the mean magnetic field and fluctuations are transverse to that direction. The correlation function for this model has the shortest scales parallel to the mean magnetic field and the longest scales perpendicular to it [*Dasso et al.*, 2005; *Osman and Horbury*, 2007]. In the quasi-two-dimensional model the excited wave vectors and magnetic field fluctuations lie in the plane perpendicular to the mean magnetic field; the correlation function has the shortest scales in the perpendicular direction and longer scales in the parallel direction [*Dasso et al.*, 2005; *Osman and Horbury*, 2007]. *Dasso et al.* [2005] and *Weygand et al.* [2009b] found that turbulent fluctuations in the slow solar wind (<450 km s^{-1}) were predominately of the quasi-two-dimensional type and those in the fast solar wind (>550 km s^{-1}) were mainly of the Alfvénic type. This effect is may be understood at least in part by noting that the turbulence in the slow wind is more compressive and "older," or more evolved, at a given

distance, compared to Alfvénic turbulence in fast wind [*Grappin et al.*, 1991].

[6] In the following sections we use our database of two spacecraft correlation data to determine the Taylor scale (λ_T) and the correlation scale (λ_{CS}) in the plasma sheet. Each type of measurement is resolved in angular channels to describe anisotropy relative to the mean magnetic field. The measurements are further subdivided into three levels of geomagnetic activity. We also derive quantitative estimates of the effective magnetic Reynolds number. Finally, we comment on cause of the variation of the correlation and Taylor scales as a function of geomagnetic activity.

2. Spacecraft and Instrumentation

[7] This study uses measurements in the plasma sheet from the multispacecraft Cluster mission. Four spacecraft provide effectively simultaneous two-point plasma and field measurements at a large range of spatial separations, enabling us to evaluate spatial correlations as a function of separation directly instead of inferring them by interpreting temporal fluctuations as frozen into a flowing plasma [*Taylor*, 1938].

[8] The Cluster mission, supported jointly by the European Space Agency (ESA) and National Aeronautics and Space Administration (NASA), consists of four identical spacecraft, optimally in a tetrahedral configuration, with a perigee of 25,500 km (4 R_E), an apogee of 125,000 km (19.6 R_E), and a spin period of about 4 s. These four spacecraft provide the first three-dimensional measurements of large- and small-scale phenomena in the near-Earth environment [*Escoubet et al.*, 1997]. Each Cluster spacecraft carries 11 instruments. The Cluster apogee precesses around the Earth annually. From 2001 to 2007, between July and October the Cluster spacecraft apogees were in the magnetotail and between January and April they were intermittently in the solar wind. At apogee in the summer seasons, the spacecraft were located at the vertices of nearly regular tetrahedrons. The scales of the tetrahedra differed from one season to the next, covering a range of distances pertinent to turbulence studies. In the magnetotail seasons of 2001 and 2004, the tetrahedron's scale was about 1000 km, which is close to the short wavelength limit of the inertial range. During the 2002 season the scale was 5000 km (i.e., on the order of the inertial range for turbulence within the plasma sheet). The latter spacing is ideal for examining turbulent eddy scale sizes that are well within the inertial range [*Neagu et al.*, 2002; *Weygand et al.*, 2005]. From July to October 2003, Cluster obtained another series of plasma sheet crossings at an interspacecraft spacing of about 100 km (i.e., on the order of dissipation range). In the magnetotail seasons of 2005 and 2006 the tetrahedral formation was not used; instead two pairs of spacecraft were separated by about 10,000 km and the separation within each pair was about 1000 km. The separation between the spacecraft pairs in the 2007 tail season was decreased to about 40 km.

[9] This study uses data from the magnetometer (FGM) [*Balogh et al.*, 1997] and the ion spectrometer (CIS) [*Rème et al.*, 1997]. Each Cluster spacecraft carries a boom-mounted triaxial fluxgate magnetometer [*Balogh et al.*, 1997]. Magnetic field vectors routinely are available at 22 Hz resolution (nominal mode). Both preflight and in-flight calibrations of the two magnetometers have been performed to produce carefully calibrated (and intercalibrated) magnetic field data. The relative uncertainty in the data after calibration is at most 0.1 nT, an estimate determined by examining the drift in the offset after calibration (K. K. Khurana and H. Schwarzl, private communication, 2004). The digital resolution of the magnetometer is on the order of 8 pT [*Balogh et al.*, 1997].

[10] Data from the CIS instrument [*Rème et al.*, 1997], along with the magnetic field data, are essential in identifying periods when Cluster enters the plasma sheet. CIS provides fundamental plasma parameters such as density, velocity vectors, the pressure tensor, and heat flux. The uncertainties in most of these quantities are not significant for this study. Although plasma data are not available from all four spacecraft, intervals in the plasma sheet can be established from the available measurements because the spacecraft are relatively close to one another.

3. Procedure and Observations

[11] For the plasma sheet analysis, we make use of intervals with a minimum of 1 h of continuous 4 s average magnetic field data. Entries and exits from the plasma sheet are identified as times when the ion temperature significantly increases or decreases. Within the plasma sheet, we require the ion density to be greater than 0.1 cm^{-3} and the magnetic field B_x component to have values between −25 and 25 nT, thereby eliminating intervals during which the spacecraft appear to enter lobe regions owing to magnetotail flapping or other phenomena. We assume that the field and plasma conditions are physically equivalent through all intervals. We do not limit the range of bulk plasma flow speed, noting that *Weygand et al.* [2009a] found that the properties of the inertial range turbulence spectrum do not vary with bulk flow speed. They found little change in the correlation scale and Taylor scale values determined from a restricted range of bulk plasma flow speeds (30–200 km s^{-1}) and the values found by combining all bulk plasma flows.

[12] Because the large-scale structure of the magnetotail field would contribute to cross-correlation values, we remove a background magnetic field determined with a cubic fit to each data interval. We excise intervals at the very center of the plasma sheet (|B| between −10 and 10 nT) because in this region the magnetic field has a small radius of curvature rendering meaningless the mean magnetic field direction.

[13] In order to establish how the average correlation and Taylor scale values depend on the angle relative to the background field, we combine many different plasma sheet intervals. In order to obtain correlation and Taylor scale values with some reliability, we adopt rather large angular bins; our angular bins for this study are as much as 30° wide. In the plasma sheet, the correlation scale is calculated to be the decay length of an exponential function ($\exp(-r_{sep}/\lambda_{CS})$ where r_{sep} is the spacecraft separation) obtained from a robust fit to all the cross-correlation coefficients at different spacecraft separations within one angular bin. The Taylor scale is found using a method based on the Richardson extrapolation technique [*Weygand et al.*, 2007]. The Taylor scale is obtained from a two step process involving a set of parabolic fits to the cross-correlation values for separations

that are increased systematically until the Taylor scale values become stable.

3.1. Observations

[14] For each selected data interval, we calculate the time-averaged cross correlation of the magnetic field vector for each of the spacecraft pairs. This correlation value is assigned to a separation distance, which is the time average of the corresponding spacecraft separation distances for that interval. Each correlation estimate is normalized by the vector variance of the magnetic field fluctuations within that interval [*Matthaeus et al.*, 2005]. By collecting normalized correlation values from a large number of suitable plasma sheet intervals, we find estimates of the variation of the correlation function with spatial separation r. All of our correlation values are obtained from Cluster spacecraft pairs in regions above or below the central plasma sheet where the mean magnetic field direction is meaningful. Figure 1 displays the correlation versus spacecraft separation for the plasma sheet. We are also fortunate to be able to include some cross-correlation values from Geotail and Wind spacecraft pairs. These points demonstrate that the correlation function approaches zero for separations on the order of 100,000 km.

[15] Figure 2 displays the distribution of the correlation values, computed by averaging over individual intervals, as a function of separations parallel to, and perpendicular to the magnetic field direction. Using the absolute value of the spacecraft separation along the perpendicular (abcissa) and parallel (ordinate) directions with respect to the mean magnetic field, we binned the data into angular bins. We use a 30° angular bin near the mean magnetic field direction and 10° angular bins for other directions. Even though we use a larger angular range for the parallel angular bin containing the mean magnetic field direction, the solid angular bin for the parallel direction is nearly equal to the other angular bins when converted to solid angles, which is about 0.14. Figure 3 shows the correlation contours calculated using all the available plasma sheet data. In order to test the stability of the angles between the mean magnetic field direction and the spacecraft separation, we subdivided each of the plasma sheet intervals into three equal subintervals and calculated the angle between the spacecraft separation vector and the mean magnetic field direction for each subinterval. We then examined the distribution of the difference of the angle between the spacecraft separation vector and the mean magnetic field direction of the entire interval and of the subintervals. The standard deviation of the distribution of the differences is 8°. This large uncertainty might call into question the stability of our correlation scales. As an additional test we have applied a uniformly distributed random number generator to the spacecraft angular position and allowed the original angular position values to vary by up to 8°. With the new angular values we rebinned the data and recalculated the correlation scales. We find that the new correlation scale values for each angular bin are the same within the uncertainties, which indicates that the standard deviation in the angular location does not strongly influence our results.

[16] The contours in Figure 3 indicate that the correlation length is longest along the mean magnetic field and shortest perpendicular to it. This feature is similar to what was found for the slow solar wind case.

[17] Table 1 lists the correlation scale (third column), Taylor scale (fifth column), and the effective magnetic Reynolds number (last column) for each of the angular bins in Figure 2. The uncertainties of the correlation scale have been determined from the residuals from the robust fit of the exponential function to the cross-correlation values and the uncertainties of the Taylor scale have been determined from the Richardson extrapolation method discussed by *Weygand et al.* [2007]. Figure 3 and Table 1 show that the correlation scale decreases systematically from the parallel to the perpendicular direction. The Taylor scale is of order 1800 km but does not vary systematically with angle. The effective magnetic Reynolds numbers are calculated using equation 2 and the uncertainty has been propagated through. The values are scattered and can be as large as ~100, but a Reynolds number of approximately 45 fits the tabulated values with their uncertainty for all angles.

[18] In order to examine the variation of the correlation scale and Taylor scale as a function of activity, we calculated the average auroral electrojet (AE) index per interval. The AE index [*Davis and Sugiura*, 1966] is used as an indicator of the level of global geomagnetic activity, and it is well correlated with the strength of the auroral electrojet currents in the Northern Hemisphere ionosphere. The AE index is the difference between the auroral electrojet upper and lower indices, which are derived from the H component (pointing toward magnetic north) from relatively well-spaced ground magnetometer stations in the Northern Hemisphere auroral zone. Our intervals have been subdivided into quiet (0–80 nT), moderate (80–200 nT), and active (>200 nT) AE conditions. These ranges of geomagnetic activity were arbitrarily selected such that approximately an equal number of correlation values (about 400 points) were available in each range of geomagnetic activity. Bin sizes of 40 nT for a histogram of the AE were selected such that bins did not straddle geomagnetic activity boundaries. Figure 4 displays the distribution of the AE for our plasma sheet intervals with only about 400 correlation values per geomagnetic activity range, we use 30° angular bins to establish correlation contours versus angle and to calculate the correlation scales and Taylor scales.

[19] Figure 5 displays the correlation contours for the three different geomagnetic activity ranges: (top) quiet, (middle) moderate, and (bottom) active. Figure 5 shows a systematic variation from correlation contours longest along the mean magnetic field and shortest perpendicular to the mean magnetic field during quiet conditions to nearly equal lengths during active conditions. Table 2 displays the correlation scale, Taylor scale, and effective magnetic Reynolds number calculated for each range of geomagnetic activity and each angular bin. For the quiet time correlation scales, the parallel correlation scale (19,500 ± 2200 km) is about twice as large as the perpendicular scale (8200 ± 600 km), but for active conditions the parallel correlation scale (13,100 ± 700) is same as the perpendicular scale (13,000 ± 2100) within the uncertainty. The moderate case shows a correlation scale anisotropy qualitatively similar to the quiet cases.

[20] The counting statistics for some of the angular bins in Table 2 are low in some cases. As an additional means of

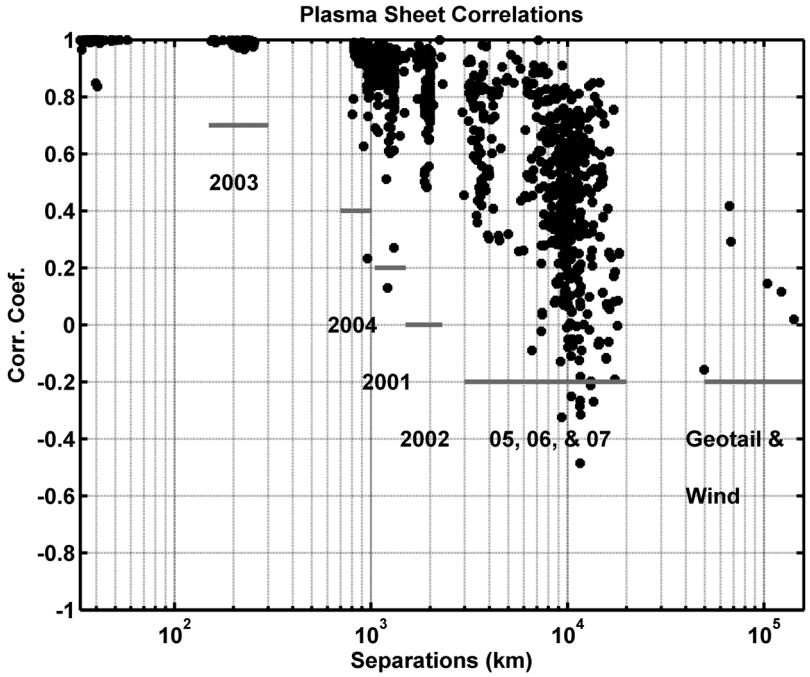

Figure 1. Spacecraft separation versus cross-correlation coefficients for the plasma sheet. Data with separations less than 20,000 km are from the Cluster spacecraft. We have indicated the years of the plasma sheet seasons that provided measurements for the approximate ranges of spacecraft separations. Larger separations were obtained from Geotail and Wind spacecraft pairs.

testing our results we examined the cross-correlation scales determined from binning the data by equally spaced solid angles cosθ, where θ is the angle between the spacecraft separation vector and the mean magnetic field direction. This method results in evenly distributed data points but creates large angular bins in the parallel direction. Nevertheless, whether we bin by angle or solid angle the results remain unchanged within one sigma.

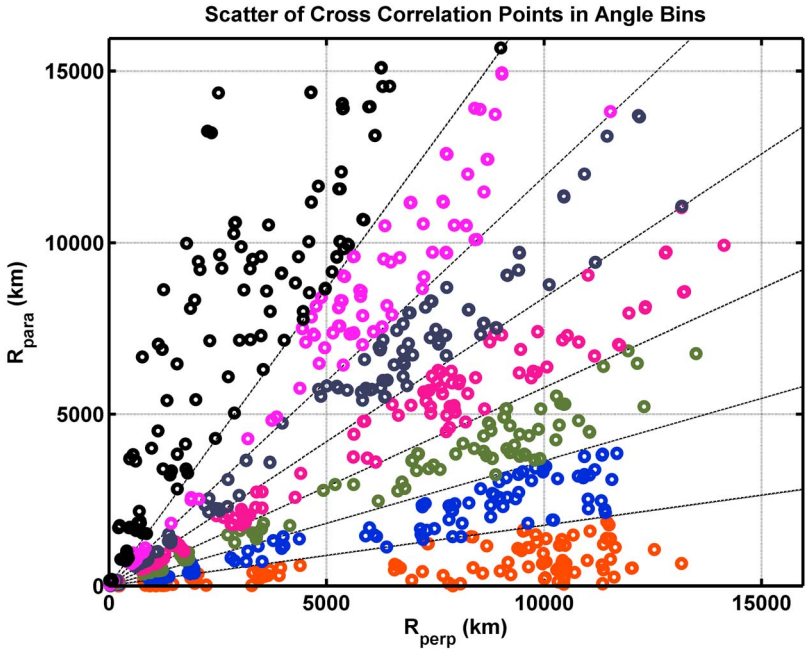

Figure 2. Distribution of spacecraft separations in the parallel and perpendicular directions with respect to the mean magnetic field direction for the plasma sheet.

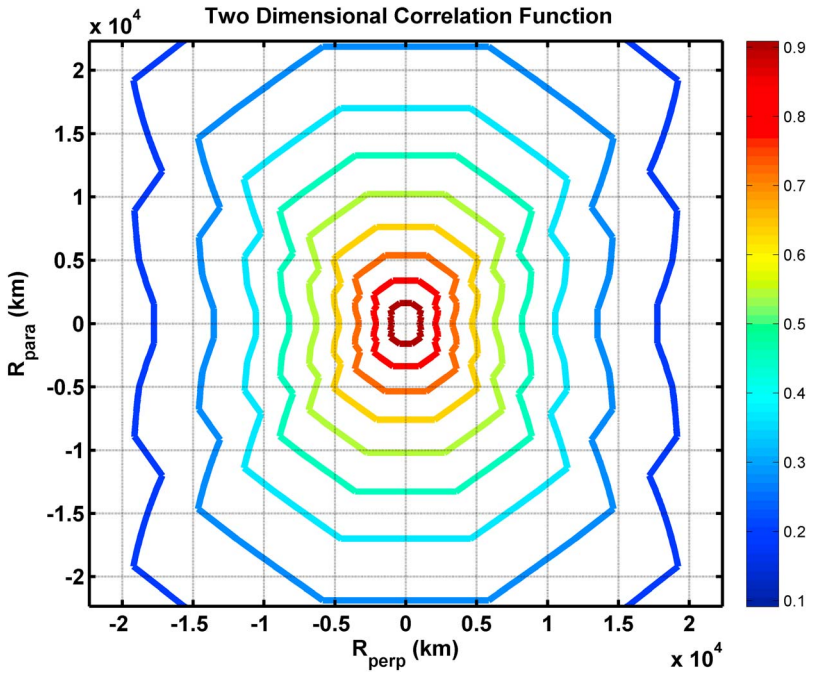

Figure 3. Correlation contour plot for the plasma sheet. The color bar indicates the cross-correlation value for each contour. Figure 3 shows that the longest correlations are along the mean magnetic field direction and the shortest correlations are in the perpendicular direction.

[21] We examined the stability of the angle between the spacecraft separation vector and the mean magnetic field direction as another test of the reliability of the smooth variation between the two dimensional cross correlation contours. During all our intervals, the spacecraft separation does not vary significantly, and we believe that during quiet geomagnetic conditions the mean magnetic field direction is stable. However, during active conditions the plasma sheet magnetic field can vary considerably. Therefore, the angle between the spacecraft separation and the magnetic field direction can also be variable. In order to test the stability of the angles between the mean magnetic field direction and the spacecraft separation, we repeated the procedure above to determine the standard deviation of the distribution of the difference of the angle between the spacecraft separation vector and the mean magnetic field direction of the entire interval and of the three subintervals. We then examined the distribution of the difference of the angle between the spacecraft separation vector and the mean magnetic field direction of the entire interval and of the subintervals. Figure 6 shows histograms of the difference in the angles for quiet, moderate, and active conditions. The histograms show that during quiet times the distribution has a small standard deviation of about 6° and, as the activity increases, the standard deviation increases up to about 10°. These small standard deviations mean that the angle between the spacecraft separation vector and the mean magnetic field direction are determined well enough that points are believably located within with only a small probability of belonging to a neighboring bin. Therefore, the isotropization seen in the correlation scale in active periods is not simply a result of ambiguity in the mean field direction. The histograms obtained from the intervals from the northern and southern plasma sheet can be further compared with the histograms plotted in Figure 7 using data obtained from the very center of the plasma sheet and containing the points we excised from our study because the magnetic field direction changes rapidly in this region. The panels in Figure 7 display broader distributions with standard deviations of 14° or

Table 1. Values of Correlation Scale, Taylor Scale, and Effective Magnetic Reynolds Number in the Plasma Sheet for the Various Angular Bins From Magnetic Field Data

Angular Range	Number of Points	λ_{CS} (km)	Number of Points	λ_{TS} (km)	Effective Magnetic Reynolds Number
0°–30°	114	16,400 ± 1000	31	2900 ± 100	30 ± 17
30°–40°	75	14,100 ± 1300	6	1700 ± 200	88 ± 59
40°–50°	98	14,800 ± 1200	19	1500 ± 200	97 ± 53
50°–60°	114	11,100 ± 700	42	2200 ± 200	28 ± 17
60°–70°	141	10,600 ± 700	51	1800 ± 100	44 ± 31
70°–80°	154	10,600 ± 600	44	1700 ± 100	50 ± 25
80°–90°	153	9200 ± 600	48	1100 ± 100	59 ± 47

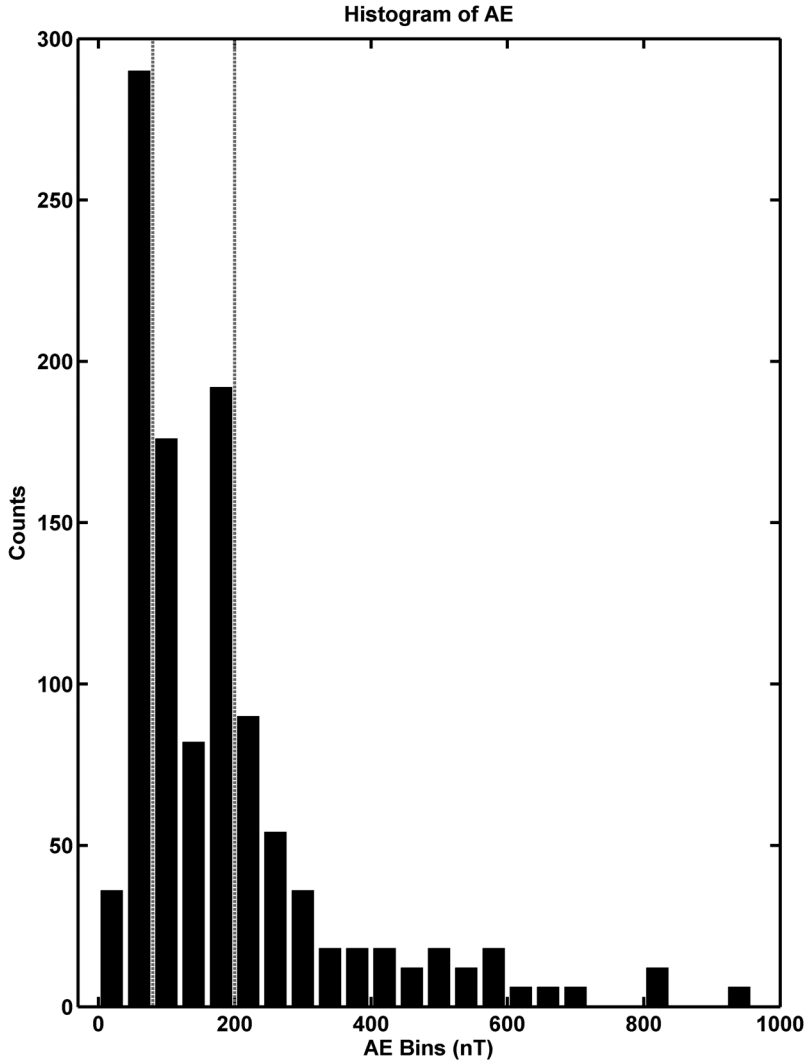

Figure 4. Histogram of the geomagnetic activity, AE index, for our plasma sheet events. The number of events per bin is given along the ordinate, and the gray lines mark the boundaries between what we have taken as quiet, moderate, and active AE ranges.

larger. These broad distributions confirm the desirability of removing these periods from our cross-correlation contours.

[22] We are confident of the rough magnitude of the Taylor scale values tabulated (~2000 km) because they are all within a factor of 3 of one another, but we are not confident of the precise values especially for the parallel direction during quiet and active geomagnetic conditions because they were obtained from fewer than 10 values. For other angular bins, the Taylor scales were obtained from a minimum of 14 or more values, but even in these angular ranges the uncertainty is still too large to allow us to say anything about a systematic change in the Taylor scale value with respect to either the mean magnetic field direction or the level of geomagnetic activity.

4. Discussion

[23] The contours of the cross-correlation functions of magnetic fluctuations as a function of the angle relative to the mean magnetic field reveal a systematic change in shape with increasing geomagnetic activity. In particular, along the mean magnetic field direction the correlation scale is longest during geomagnetically quiet intervals and decreases with increasing geomagnetic activity. On the other hand, the correlation scales in the perpendicular direction and in the 30°–60° bin systematically increase with increasing geomagnetic activity. The correlation scale becomes nearly isotropic in the active intervals, while the Taylor scale retains some of the anisotropy that is seen more strongly in the quiet intervals.

[24] We consider two possible reasons for this systematic change of scale length and its dependence on angle: changes of the nature of the structures that drive the turbulent fluctuations and changes of the nature of the turbulent fluctuations themselves. Both of these may vary with geomagnetic activity and with angle relative to the mean magnetic field.

[25] Consider first how the form of the driving structures may depend on the level of geomagnetic disturbance.

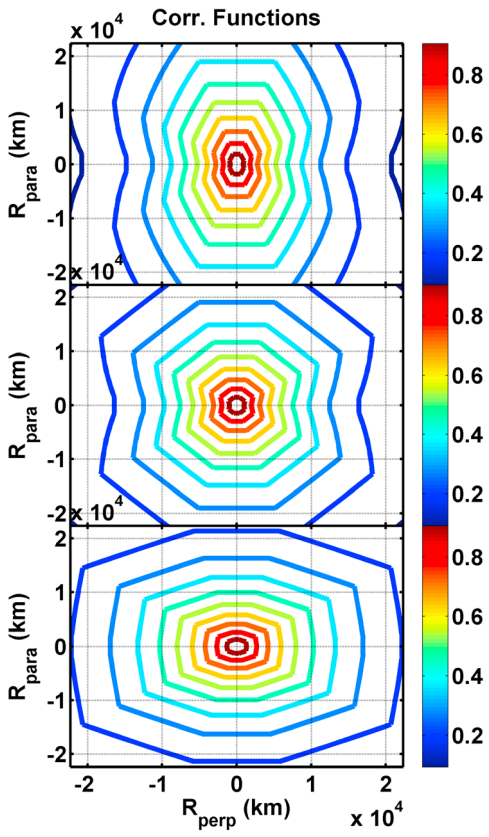

Figure 5. Two-dimensional plasma sheet correlation function contours for (top) quiet, (middle) moderate, and (bottom) active geomagnetic conditions. The plots show a systematic change in the correlation scales of the plasma sheet from quiet to active conditions.

During quiet geomagnetic intervals, flow shears tend to be well developed and to stretch along the mean magnetic field direction. Figure 8 is a cross section of flow and mean magnetic field magnitude in the plasma sheet from an MHD model [*El-Alaoui*, 2001; *El-Alaoui et al.*, 2008; *Raeder et al.*, 1995, 2001] run for northward interplanetary magnetic field (IMF) conditions and consequently geomagnetically quiet. In Figure 8 the vectors represent the flow velocity, the colors indicate the value of the B_z component of the magnetic field, the solar wind comes from the Sun on the left side of Figure 8, and the black contours indicate curves of constant pressure. Shear flows are on average aligned along the *X*-GSM axis, such as the long shear flow at about (−20, −5) R_E and another at (−20, 7.5) R_E that extends mostly along the *X* direction, and a few weak vortices are evident at (−31, −2) R_E and (−8, 10) R_E. In Figure 9, from a run of the same model during southward IMF and correspondingly active geomagnetic conditions, the flow shears seem shorter, wavy, and less aligned with the *X*-GSM axis such as those at (−20, 8) R_E and (−20, −5) R_E, and more developed vortical flows are found in the plasma sheet like those at (−16, 2.5) R_E, (−18, 2.5) R_E, and (−22, −9) R_E. This difference in the length and shape of the flow shears was well as the number and strength of the vortices suggests there is a change of the nature of the structures that drive the turbulent fluctuations.

[26] Testing this interpretation would be difficult with spacecraft observations because we would need many more spacecraft over a large range of *X* and *Y* locations in order to more clearly identify the scale sizes of the shear and vortical flows. However, this interpretation could be done by examining instantaneous images of the flow and vortices sizes from simulations. With a number of observations of the plasma sheet from the simulations the length, alignment, and number of shear flows and vortices could be determined for each level of geomagnetic activity. We hypothesize that during quiet conditions the length of the shear flows would be longer and more likely to be aligned with the *X*-GSM axis, but the number of shear flows and vortices would be greater during active conditions. The longer shear flows and alignment with the X-GSM axis during quiet conditions should produce the long correlation scale along the mean magnetic field and shorter scale perpendicular to the field. During active conditions the short shear flows and more numerous vortices should produce the short and isotropic correlation contours. In principle, two-dimensional correlation contours can be produced from the MHD magnetic field vectors in the simulation, for comparison with the observations. However, we defer this time-consuming task for future study.

[27] An alternative explanation for the variation in the length of the correlation scale with geomagnetic activity and its dependence on angle with respect to the average magnetic field direction may be related to the dominance of different sources of the turbulent magnetic field fluctuations. *Dasso et al.* [2005] demonstrated that at least two types of magnetic field turbulence are present within the solar wind.

Table 2. Correlation Scale, Taylor Scale, and Effective Magnetic Reynolds Number Determined for Each Angular Bin for the Three Different Ranges of Geomagnetic Activity

	Angular Bin	Num. of Points	Correlation Scale (km)	Number of Points	Taylor Scale (km)	Effective Magnetic Reynolds Number
Quiet AE 0–80 nT	0°–30°	46	19,500 ± 2200	8	6000 ± 700	11 ± 7
	30°–60°	97	11,700 ± 1000	16	900 ± 50	169 ± 90
	60°–90°	136	8200 ± 600	57	800 ± 300	105 ± 100
Moderate AE 80–200 nT	0°–30°	50	15,100 ± 1300	14	2500 ± 400	36 ± 25
	30°–60°	119	13,000 ± 900	40	1000 ± 800	169 ± 216
	60°–90°	188	9600 ± 500	61	1700 ± 140	32 ± 17
Active AE 200–1000 nT	0°–30°	144	13,100 ± 700	9	4000 ± 1600	11 ± 10
	30°–60°	93	14,900 ± 1100	14	2000 ± 1000	56 ± 58
	60°–90°	23	13,000 ± 2100	26	1400 ± 100	86 ± 57

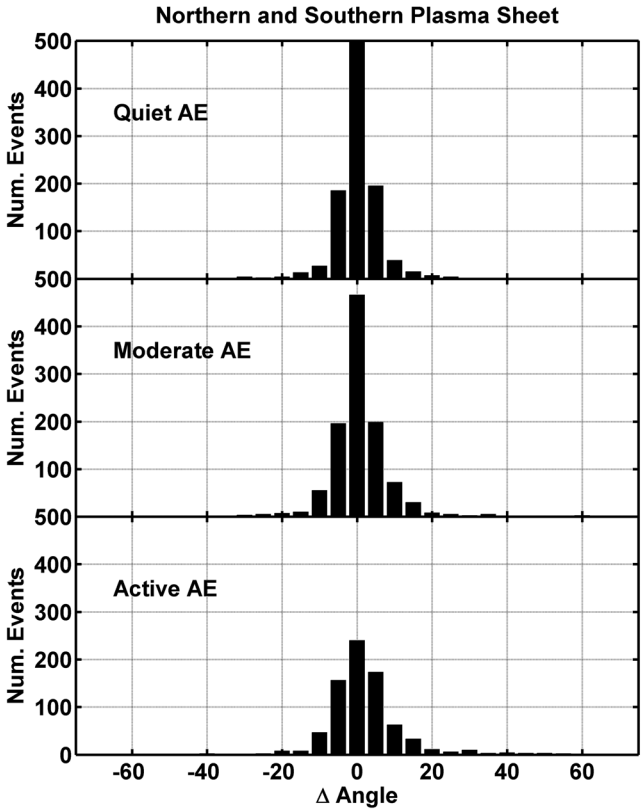

Figure 6. Histogram of the difference in angle between the angle determined from each interval and the angles determined from each subinterval for the northern and southern plasma sheet intervals used to make the two-dimensional cross-correlation contours.

The two types can be best observed by separating solar wind data into intervals for which the flow speed is slow (<400 km s^{-1}) and fast (v_{sw} > 500 km s^{-1}). In the slow solar wind, it has been shown that the correlation scales are longest parallel to the mean magnetic field and shortest perpendicular to the mean magnetic field direction. This structure has been attributed to the dominance of quasi two-dimensional fluctuations in the slow solar wind [*Dasso et al.*, 2005; *Weygand et al.*, 2009a]. In the fast solar wind, Alfvénic type fluctuations are more prominent and the correlation scales are longest perpendicular to the mean magnetic field direction and shortest along the magnetic field [*Dasso et al.*, 2005].

[28] It is possible that the change of shape with activity shown in Figure 5 arises from different types of turbulence. During quiet intervals, the correlation contours are stretched along the magnetic field and most resemble solar wind correlation contours thought to result from quasi two-dimensional fluctuations where the wave vectors and magnetic field perturbations are in the plane perpendicular to the magnetic field direction [*Dasso et al.*, 2005; *Weygand et al.*, 2009b]. These turbulent fluctuations may be magnetosonic waves generated by velocity shears and vortices where we assume that the size of the shear is on the order of the driver of the turbulent magnetic field fluctuations. As geomagnetic activity increases, the Alfvénic fluctuations become more important. It has been proposed that Alfvén waves can produced by mode conversion from compressional waves in the plasma sheet [*Lee et al.*, 2001], due to twisting of magnetic field lines [*Song and Lysak*, 2001], bursty bulk flows [*Angelopulos et al.*, 2002], and magnetic field line reconnection. Many of these processes are believed to occur more frequently during active conditions. However, we emphasize that both quasi two-dimensional fluctuations and Alfvénic turbulent fluctuations are still present at all levels of geomagnetic activity. In fact, *Volwerk et al.* [2003] have demonstrated that the total power associated with quasi two-dimensional turbulence increases with increased plasma sheet activity.

[29] Our correlation contours seen in Figure 5 could be understood if one type of turbulence dominates over the other when the magnetosphere is relatively quiet, but the balance between the types of turbulent fluctuations changes when the magnetosphere becomes more active. Such a change in the nature of turbulent fluctuations could result if the dominant wave mode present in the plasma sheet depends on the level of activity. It is not unreasonable to believe that during high levels of activity, Alfvénic turbulence is continually produced by magnetic field line twisting, bursty bulk flows, and reconnection and the power generated balances or exceeds the loss to the ionosphere. We expect the total Alfvénic turbulence power to increase with increasing geomagnetic activity as shown by *Volwerk et al.* [2003]. Thus, it is possible that the rate of increase of power with activity is higher for Alfvénic turbulence than

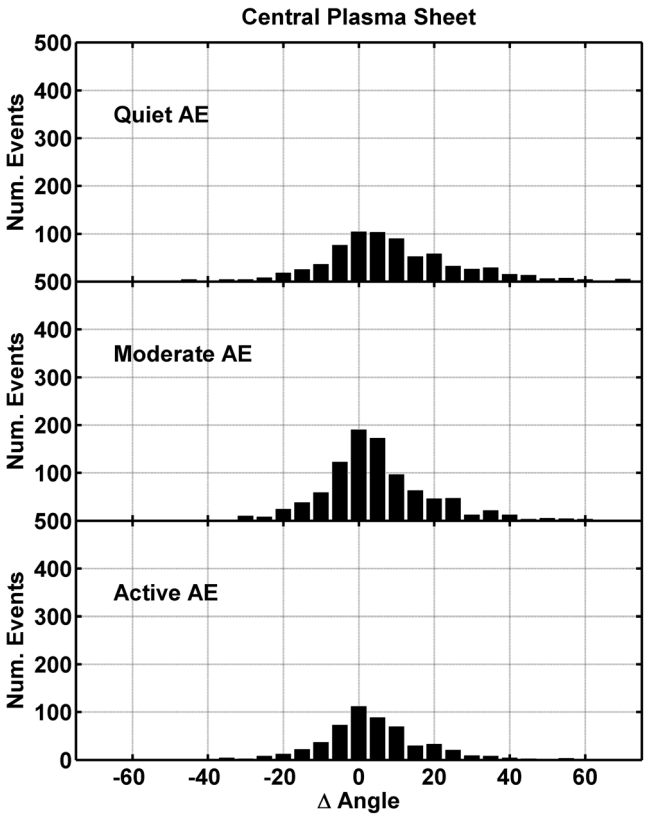

Figure 7. Same format as in Figure 6 and was created using magnetic field data from the central plasma sheet.

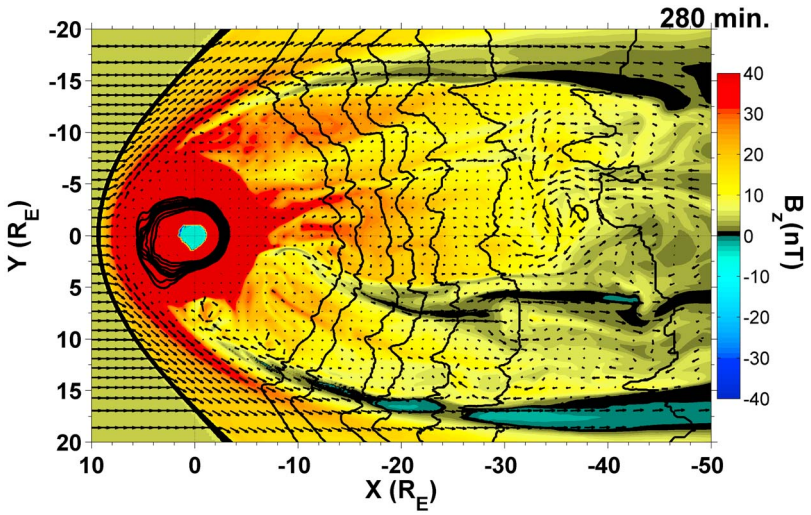

Figure 8. From an MHD simulation [*Alaoui et al.*, 2008; *Raeder et al.*, 1995, 2001]. Model flow vectors, Bz values in color, and constant pressure contours (black curves) for the plasma sheet during northward IMF and geomagnetically quiet conditions.

for quasi two-dimensional turbulence. However, it is also possible that the increase of power with activity is the same for different wave modes but that the rate at which the ionosphere damps Alfvénic modes decreases with activity. Such a proposal is plausible because the nightside auroral zone conductance increases with activity. At quiet times, Alfvén waves are highly damped in the dark hemisphere, possibly even within one wave cycle. At disturbed times, precipitation into the ionosphere increases its conductivity and reduces the damping rate of Alfvénic perturbations, thereby allowing Alfvénic perturbations to persist for multiple cycles.

[30] Another important feature to take note of is the finite scale size of the plasma sheet in the *Z*-GSM direction compared to the perpendicular correlation scale length. If the magnetic field turbulence is bound within the plasma sheet, then the correlation scale in the perpendicular direction should not exceed a typical plasma sheet thickness. Typical plasma sheet thicknesses are on the order of 6400–25,600 (1–4 R_E). Tables 1 and 2 show that we have perpendicular correlation scale lengths on the order of 8200–13,000 km, which are within the range of plasma sheet thicknesses given. Our perpendicular correlation scales, however, do not differentiate between the *Z* and the *Y*-GSM direction (i.e., the two directions in the plasma sheet that are generally perpendicular to the mean magnetic field direction in the northern and southern plasma sheet regions) and our perpendicular scales will be an average perpendicular length. *Weygand et al.* [2005] demonstrated, however, using Cluster observation of turbulent plasma sheet magnetic field fluctuation data that the autocorrelation scale lengths in the *Y* direction were on average shorter than the *Z* direction, which suggests that our perpendicular correlation scales fit within the plasma sheet. Furthermore, as discussed in

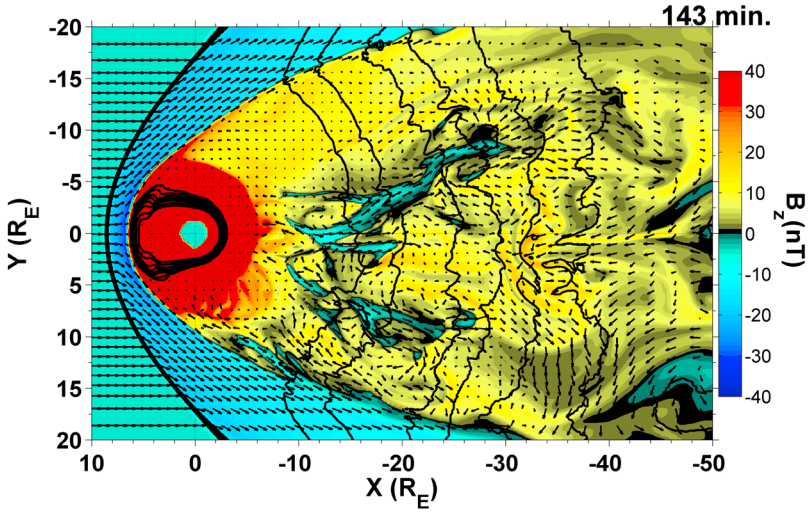

Figure 9. Same format as in Figure 8, MHD model flow vectors, Bz values, and constant pressure contours for the plasma sheet region during southward IMF and geomagnetically active conditions.

section 3, we have tried to be conservative in the selection of our plasma sheet intervals and are confident that we have not included intervals that are outside of the plasma sheet. In other words, the mean perpendicular correlation scale we report here should be considered to be less than the mean plasma sheet thickness.

[31] Whereas the correlation scales vary systematically with the geomagnetic activity, the Taylor scale values do not. However, many of our estimates of the Taylor scales have large uncertainties. These large uncertainties are possibly the result of poor statistics and only with the addition of more intervals can the dependence on magnetic activity be tested. However, our results here are similar to those of *Weygand et al.* [2009a], who found that the Taylor scale was largest along the mean magnetic field and relatively constant for angular bins larger than 30°. That study suggested that the anisotropy observed in the Taylor scales may be linked to the anisotropy of the inertial range fluctuations and their interaction with the mean magnetic field [*Oughton and Matthaeus*, 2005], but also could arise from anisotropy of dispersive and dissipative effects, including Landau damping, cyclotron resonance, kinetic Alfvén waves, and other processes that depend upon the direction of the magnetic field [*Leamon et al.*, 1999; *Gary and Borovsky*, 2004].

[32] In the last column of Table 2, the effective magnetic Reynolds numbers in the plasma sheet within the inertial range for the three different levels of geomagnetic activity are calculated from the Taylor and correlation scales. The effective magnetic Reynolds numbers vary between 11 and 169 with a mean value of 75. However, no one Reynolds number can be given that would fall within the uncertainties for all angles and levels of geomagnetic activity. More data intervals are required to improve the statistics in order to establish more clearly whether or not the Reynolds number varies with the mean magnetic field direction. The effective magnetic Reynolds numbers found here are similar to the range of values (7–110) reported by *Weygand et al.* [2007] and (28–97) reported by *Weygand et al.* [2009a].

5. Conclusions

[33] In this study we found that the correlation scales vary with respect to the mean magnetic field direction for different levels of geomagnetic activity. As far as we are aware this is the first study to establish this feature. Using the Taylor scale and the correlation scale, we derived the effective magnetic Reynolds number for each angular bin. In the plasma sheet the effective magnetic Reynolds number shows some variability with the angle relative to the magnetic field, but remains within 2 standard deviations of a constant value. The uncertainties of our analysis are considerable and could be reduced by addition of many more events in order to establish the relation between the effective magnetic Reynolds number and the angle relative to the magnetic field. The value of the magnetic Reynolds number and its possible anisotropy are important parameters for numerical MHD models.

[34] Our results show that plasma sheet turbulence is anisotropic at both low and moderate levels of geomagnetic activity, but we have not established why the nature of the anisotropy changes with activity. We have proposed that the structures driving turbulence may change form with geomagnetic activity and have also suggested that quasi two-dimensional turbulence may dominate Alfvénic turbulence during quiet periods, but the balance may change as the plasma sheet responds to geomagnetic activity. Since different dominant forms of turbulence have been identified in the fast and slow solar wind, the predominant type of magnetic field turbulence in the plasma sheet may differ at different levels of geomagnetic activity.

[35] While the specific causes of change in anisotropy are uncertain at present, it seems clear that the quiet intervals exhibit greater large-scale anisotropy than is seen in the active intervals. This is consistent with the general statement that the driving of the turbulence in the active intervals may be relatively more isotropic and less sensitive to the mean magnetic field direction, though perhaps depending on factors such as shears and vortical flows. In contrast, the Taylor scale, which reflects less on of driving and more of local turbulence properties, retains in the active intervals a greater degree of anisotropy than does the correlation scale. A variety of specific mechanisms, some suggested above, may be consistent with this picture.

[36] As a final remark, we note that the fact that the variation of correlation and Taylor scales with respect to the mean magnetic field direction should be recognized in the analysis of particle scattering within the magnetosphere because the perpendicular diffusion coefficient is directly proportional to the correlation scale [*Ruffolo et al.*, 2004], while the parallel scattering rate depends on anisotropy in the inertial range [*Bieber et al.*, 1994].

[37] **Acknowledgments.** This work was supported by NASA grant NAG5-12131 at UCLA. W.H. Matthaeus is partially supported by NSF grants ATM-0539995 and ATM0752135 (SHINE) and by NASA NNX08AI47G and NNG05GG83G at the University of Delaware. S. Dasso thanks the Argentinean grants UBACyT X425 (UBA) and 03-33370 (ANPCyT). S. Dasso is a member of the Carrera del Investigador Científico (CONICET). We would like to thank M.L. Goldstein, J.E. Borovsky, P. Chuychai, and Z. Vörös for their helpful discussions. We would also like to thank H. Schwarzl and K.K. Khurana for calibrating the Cluster magnetometer data and their advice on the calibration process. Finally, we thank E. Lucek for providing UCLA with the Cluster magnetometer data and L. Kistler for providing us with the Cluster CIS data.

[38] Philippa Browning thanks the reviewers for their assistance in evaluating this paper.

References

Angelopulos, V. J., A. Chapman, F. S. Mozer, J. D. Scudder, C. T. Russell, K. Tsuruda, T. Mukai, T. J. Hughes, and K. Yumoto (2002), Plasma sheet power generation and its dissipation along auroral field lines, *J. Geophys. Res.*, *107*(A8), 1181, doi:10.1029/2001JA900136.

Balogh, A., et al. (1997), The Cluster magnetic field investigation, *Space Sci. Rev.*, *79*, 65–91.

Batchelor, G. K. (1970), *Theory of Homogeneous Turbulence*, Cambridge Univ. Press, Cambridge, U. K.

Bieber, J. W., W. H. Matthaeus, C. W. Smith, W. Wanner, M.-B. Kallenrode, and G. Wibberenz (1994), Proton and electron mean free paths: The Palmer consensus revisited, *Astrophys. J.*, *420*, 294–306.

Borovsky, J. E., R. C. Elphic, H. O. Funsten, and M. F. Thomsen (1997), The Earth's plasma sheet as a laboratory for turbulence in high-beta MHD, *J. Plasma Phys.*, *57*, 1–34.

Dasso, S., L. J. Milano, W. H. Matthaeus, and C. W. Smith (2005), Anisotropy in fast and slow solar wind fluctuations, *Astrophys. J.*, *635*, L181–L184.

Davis, T. N., and M. Sugiura (1966), Auroral electrojet index AE and its universal time variations, *J. Geophys. Res.*, *71*(3), doi:10.1029/JZ071i003p00785.

El-Alaoui, M. (2001), Current disruption during November 24, 1996, substorm, *J. Geophys. Res.*, *106*(A4), 6229–6245, doi:10.1029/1999JA000260.

El-Alaoui, M., M. Ashour-Abdalla, J. M. Bosqued, and R. L. Richard (2008), Understanding Magnetotail current sheet meso-scale structures using MHD simulations, *Adv. Space Res.*, doi:10.1016/j.asr.2007.05.061.

Escoubet, C. P., R. Schmidt, and M. L. Goldstein (1997), Cluster-science and mission overview, *Space Sci. Rev.*, *79*, 11–32.

Gary, S. P., and J. E. Borovsky (2004), Alfvén-cyclotron fluctuations: Linear Vlasov theory, *J. Geophys. Res.*, *109*, A06105, doi:10.1029/2004JA010399.

Goldstein, M. L., D. A. Roberts, and C. A. Fitch (1994), Properties of the fluctuating magnetic helicity in the inertial and dissipation ranges of solar wind turbulence, *J. Geophys. Res.*, *99*(A6), 11,519–11,538, doi:10.1029/94JA00789.

Goldstein, M. L., D. A. Roberts, and W. H. Matthaeus (1995), Magnetohydrodynamic turbulence in the solar wind, *Annu. Rev. Astron. Astrophys.*, *33*, 283–325.

Grappin, R., M. Velli, and A. Mangeney (1991), "Alfvenic" versus "standard" turbulence in the solar wind, *Ann. Geophys.*, *9*, 416–426.

Kolmogorov, A. N. (1941), The local structure of turbulence in incompressible viscous fluid for very large Reynolds' numbers, *Dokl Akad Nauk SSSR*, *30*, 301–305.

Kraichnan, R. H. (1965), Inertial-range spectrum of hydromagnetic turbulence, *Phys. Fluids*, *8*, 1385–1387.

Leamon, R. J., C. W. Smith, N. F. Ness, and H. K. Wong (1999), Dissipation range dynamics: Kinetic Alfvén waves and the importance of β_e, *J. Geophys. Res.*, *104*(A10), 22,331–22,344, doi:10.1029/1999JA900158.

Lee, D.-H., R. J. Lysak, and Y. Song (2001), Generation of field-aligned currents in the near-Earth magnetotail, *Geophys. Res. Lett.*, *28*(9), 1883–1886, doi:10.1029/2000GL012202.

Matthaeus, W. H., M. L. Goldstein, and D. A. Roberts (1990), Evidence for the presence of quasi-two-dimensional nearly incompressible fluctuations in the solar wind, *J. Geophys. Res.*, *95*(A12), 20,673–20,683, doi:10.1029/JA095iA12p20673.

Matthaeus, W. H., S. Dasso, J. M. Weygand, L. J. Milano, C. W. Smith, and M. G. Kivelson (2005), Spatial correlation of the solar wind turbulence from two point measurements, *Phys. Rev. Lett.*, *95*, 231101.

Matthaeus, W. H., J. M. Weygand, P. Chuychai, S. Dasso, C. W. Smith, and M. G. Kivelson (2008), Interplanetary magnetic Taylor scale and implications for plasma dissipation, *Astrophys. J.*, *678*, L141–L144.

Neagu, E., J. E. Borovsky, M. F. Thomsen, S. P. Gary, W. Baumjohann, and R. A. Treumann (2002), Statistical survey of magnetic and velocity fluctuations in the near-Earth plasma sheet: AMPTE/IRM measurements, *J. Geophys. Res.*, *107*(A7), 1098, doi:10.1029/2001JA000318.

Osman, K. R., and T. S. Horbury (2007), Multispacecraft measurement of anisotropic correlation functions in the solar wind turbulence, *Astrophys. J.*, *654*, L103–L106.

Oughton, S., and W. H. Matthaeus (2005), Parallel and perpendicular cascades in solar wind turbulence, *Nonlinear Process. Geophys.*, *12*, 299–310.

Raeder, J., R. J. Walker, and M. Ashour-Abdalla (1995), The structure of the distant geomagnetic tail during long periods of northward IMF, *Geophys. Res. Lett.*, *22*(4), 349–352, doi:10.1029/94GL03380.

Raeder, J., R. L. McPherron, L. A. Frank, S. Kokubun, G. Lu, T. Mukai, W. R. Paterson, J. B. Sigwarth, H. J. Singer, and J. A. Slavin (2001), Global simulation of the Geospace Environment Modeling substorm challenge event, *J. Geophys. Res.*, *106*(A1), 381–396, doi:10.1029/2000JA000605.

Rème, H., et al. (1997), The Cluster ion spectrometry (CIS) experiment, *Space Sci. Rev.*, *79*, 303–350.

Ruffolo, D., W. H. Matthaeus, and P. Cuychai (2004), Separation of magnetic field lines in two-component turbulence, *Astrophys. J.*, *614*, 420–434.

Song, Y., and R. L. Lysak (2001), The physics in the auroral dynamo regions and auroral particles acceleration, *Phys. Chem. Earth*, *26*, 33–42.

Taylor, G. I. (1938), The spectrum of turbulence, *Proc. R. Soc., Ser A*, *164*, 476–490.

Tu, C. Y., and E. Marsch (1995), MHD structures, waves and turbulence in the solar wind, *Space Sci. Rev.*, *73*, 1–210.

Volwerk, M., et al. (2003), A statistical study of compressional waves in the tail current sheet, *J. Geophys. Res.*, *108*(A12), 1429, doi:10.1029/2003JA010155.

Weygand, J. M., M. G. Kivelson, K. K. Khurana, H. K. Schwarzl, R. J. Walker, A. Balogh, L. M. Kistler, and M. L. Goldstein (2006), Non-self similar scaling of plasma sheet and solar wind probability distribution functions of magnetic field fluctuations, *J. Geophys. Res.*, *111*, A11209, doi:10.1029/2006JA011820.

Weygand, J. M., et al. (2005), Plasma sheet turbulence observed by Cluster II, *J. Geophys. Res.*, *110*, A01205, doi:10.1029/2004JA010581.

Weygand, J. M., W. H. Matthaeus, S. Dasso, M. G. Kivelson, and R. J. Walker (2007), Taylor scale and effective magnetic Reynolds number determination from the plasma sheet and the solar wind magnetic field fluctuations, *J. Geophys. Res.*, *112*, A10201, doi:10.1029/2007JA012486.

Weygand, J. M., W. H. Matthaeus, S. Dasso, and M. G. Kivelson (2009a), Anisotropy of the Taylor scale and the correlation scale in plasma sheet and solar wind magnetic field fluctuations, *J. Geophys. Res.*, *114*, A07213, doi:10.1029/2008JA013766.

Weygand, J. M., M. G. Kivelson, W. H. Matthaeus, S. Dasso, and L. M. Kistler (2009b), Anisotropies of the Taylor scale, correlation scale, and effective magnetic Reynolds number determination from solar wind magnetic field fluctuations, paper presented at the European Geophysical Union Conference, Vienna, Austria, April.

S. Dasso, Instituto de Astronomía y Física del Espacio (IAFE) and Departmento de Física, Facultad de Ciencias Exactas y Naturales, Universidad de Buenos Aires, CC67 Suc. 28, 1428 Buenos Aires, Argentina.

M. El-Alaoui, M. G. Kivelson, and J. M. Weygand, Institute of Geophysics and Planetary Physics, University of California, 3845 Slichter Hall, 405 Charles E. Young Dr., Los Angeles, CA 90095, USA. (jweygand@igpp.ucla.edu)

W. H. Matthaeus, Bartol Research Institute, Department of Physics and Astronomy, 217 Sharp Laboratory, University of Delaware, Newark, DE 19716, USA.